

Aero-Thermal Optimization of Internally Cooled Turbine Blades

George S. Dulikravich ¹, Thomas J. Martin ² and Zhen-Xue Han ³

Abstract. A quasi-conjugate approach to automatic constrained optimization design of internally cooled gas turbine blades has been developed. Design parameters involve sizes, shapes, and locations of internal coolant flow passages, thickness variation of the blade wall and thermal barrier coatings, average surface roughness of the coolant passage walls, inlet gas temperature, and coolant supply pressure. The objective is to make temperature distribution in the blade material as uniform as possible. Preliminary computational results demonstrate possibilities to design blades with significantly higher inlet hot gas temperatures while requiring remarkably lower coolant mass flow rates and having reduced thermal gradients. The methodologies discussed in this paper were chosen because they have been perceived to be the most robust and computationally affordable.

1 INTRODUCTION

The objective of this paper is to sketch a multidisciplinary design procedure that is capable of maximizing inlet turbine temperature, and enhancing the uniformity of temperature field in the blade material, while at the same time minimizing coolant mass flow rate, inlet-to-exit total pressure loss, and coolant supply pressure.

We will consider aerodynamics of the hot gas flow in detail, coolant aerodynamics and heat transfer

very approximately, heat conduction in the blade material very accurately. These individual disciplines will not be solved simultaneously because this approach would take an unacceptably long time even on a cluster of workstations running in parallel. For these pragmatic reasons we opted for a computationally affordable sequential, loosely coupled, design approach as follows [1].

First, an initial realistic shape of a turbine blade was generated and the hot gas flow-field around it was analyzed using computational fluid dynamics (CFD) [2]. Then, if an aerodynamic performance improvement was desired, an inverse shape design of the blade was performed subject to the desired surface pressure distribution while accounting for fluid compressibility, heat transfer, and turbulence. If the aerodynamic performance was to be maximized, the blade shape was optimized subject to constraints such as fixed axial chord length, inlet and exit flow angles, minimum allowable trailing edge radius, and hot gas mass flow rate [1].

2 THERMAL SHAPE OPTIMIZATION

The first step in the design of the multiple coolant flow passages was the description of the airfoil wall thickness. The coating thickness distribution was described using the β -splines so that it varied from point to point along the airfoil contour [3].

Figure 1 illustrates the complete geometric modeling of the coolant flow passages and thermal barrier coating. The range over which each strut's end-points could vary was specified and the number of coolant flow passages in the turbine airfoil was specified. In addition to the end-coordinates of the struts, the strut thickness and a filleting L

¹ Associate Professor, Department of Aerospace Engineering, 233 Hammond Bldg., The Pennsylvania State University, University Park, PA 16802, U.S.A.

² Graduate Research Assistant, Department of Aerospace Engineering, 233 Hammond Bldg., The Pennsylvania State University, University Park, PA 16802, U.S.A.

³ Visiting Scholar, Associate Professor, BUAA, Beijing, China.

curve exponents on the pressure and suction sides were used to complete the geometric modeling of each strut (Figs. 1 and 2).

At present, the computational time needed for a fully coupled three-dimensional conjugate analysis is still too long for numerical optimization purposes. Therefore, a simpler semi-conjugate heat transfer analysis and optimization of the turbine blade was developed. The application of thermal boundary conditions on the coolant flow passage walls was greatly simplified by the specification of convective heat transfer coefficients and ambient fluid temperatures of the coolant fluid.

$$q'' = -k_M \frac{\partial T}{\partial n} = h_{cool,n} (T_w - T_{cool,n}) \quad (1)$$

Here, k_M is the coefficient of thermal conductivity of the metal blade. The convective heat transfer coefficient, h_{cool} , on the walls of the n th coolant passage was allowed to vary with the following parameters: velocity of the coolant, V_{cool} , coolant density, ρ_{cool} , the hydraulic diameter of the passages, D_h , temperature of the passage wall, T_w , bulk temperature of the coolant, T_{cool} , average wall roughness height, ϵ . This list of variables was replaced by non-dimensional variables which were all based upon the bulk coolant flow properties [4, Chapter 5].

The non-dimensional numbers are: Stanton number, Reynolds number, Prandtl number, Eckert number, Nusselt number, and friction factor, f .

The temperature gradients in the coolant were assumed to be small enough to eliminate temperature-dependent physical properties. Thermal buoyancy and viscous dissipation effects were neglected as were the centripetal and Coriolis acceleration effects. The Reynolds analogy is often used to produce a solution under these circumstances.

$$StPr^{0.667} = \frac{f}{8} \quad (2)$$

The friction factor, f , was related to the pressure loss in the coolant passage by the well-known formula for fully developed pipe flows driven only by the pressure gradient.

The value of the local friction factor could be taken from the Moody chart knowing the relative surface roughness, ϵ/D , of the particular section of the coolant passage and the corresponding local Reynolds number [5, p. 230]. For optimization purposes, the friction factor should be allowed to

change during the optimization process. Therefore, an explicit formula given by Haaland was used [6]

$$\frac{1}{f^{1/2}} = -1.8 \log_e \left[\frac{6.9}{Re_D} + \left(\frac{\epsilon/D}{3.7} \right)^{1.11} \right] \quad (3)$$

This explicit expression is accurate to within 2% of the Moody chart, which itself is accurate to +/-15% versus experimental data for fully turbulent flows. During the numerical optimization procedure, the relative wall roughness in the turbulent flow coolant passage was a design variable that was allowed to increase up to $\epsilon/D = 0.15$. Large relative wall roughness values simulated the effect of placing pin fins and trip strips on the coolant passage walls. These heat transfer correlations were based on the local hydraulic diameters of the coolant passages. Given the coolant mass flow rate, $\dot{m} = \rho_{cool} A_h V_{cool}$, the local average velocity of the coolant and the corresponding local Reynolds numbers were computed.

The coolant mass flow rate was allowed to vary during the optimization process so that it could be correlated with the limiting temperature on the hot surface of the turbine blade. Only the inlet coolant fluid temperature was specified and kept fixed.

The coolant streamwise pressure gradients were calculated for each coolant passage section given the empirical relationships previously described, $dp/dz = \Delta p/L$. These pressure gradients were used to determine the minimum required coolant supply pressure. That is, the static pressure, p_{cool} , at the inlet of the first coolant flow passage (at the root of the blade leading edge) was determined given the pressure losses in the entire coolant passage and the knowledge of a fixed static pressure, p_{static} , at the exit of the last coolant flow passage segment (assumed to be equal to the hot gas pressure at the blade trailing edge). Because the relationship between the coolant pressure loss and coolant inlet pressure was implicit, the bisection method was used to determine the root of the following function.

$$p_{eject}(\dot{m}, \epsilon/D, p_{cool}) - p_{static} = 0 \quad (4)$$

In this equation, the ejection static pressure, p_{eject} , was calculated given an initial guess to p_{cool} and the computed pressure losses, Δp . It was a function of the coolant mass flow rate, the coolant passage wall relative roughness, the inlet coolant pressure,

as well as the blade and coating material properties and coolant passage geometry.

The ambient (bulk) coolant temperatures in each of the coolant passages were allowed to be a non-linear function of heat flux, $T_{cool} = T_{cool}(Q)$. A quasi one-dimensional, steady state, incompressible, thermal energy equation was used to determine the bulk coolant temperatures and pressures along the entire length of the serpentine coolant flow passage.

$$\int \dot{m} c_p \frac{dT_{cool}}{dz} dz = \int \int Q ds dz + \int \frac{\dot{m}}{\rho_{cool}} \frac{\Delta p}{T_N} dz \quad (5)$$

Here, Q is the heat flux through the coolant passage walls, s is the contour-following variable along the coolant wall perimeter, and z is the coolant streamwise direction. This equation was written for each coolant passage including 180 degree turn sections and solved for the local streamwise temperature gradients, $(dT_{cool}/dz)_N$. For this purpose, we used blade outer hot surface temperatures and heat fluxes that were previously computed by the CFD analysis of the hot gas flow-field. Because T_{cool} is a function of Q , the solution of the heat conduction equation in the blade material was non-linear due to the heat flux dependent ambient coolant temperature in the convection heat transfer boundary conditions. Subsequent solutions to the heat conduction provided better estimates of the heat flux, Q , and the iterative scheme proceeded until the computed heat fluxes converged. This was typically accomplished in a maximum of five solutions of the heat conduction problem in the entire airfoil.

This simplified approach to conjugate heat transfer did not fully account for all of the heat transfer characteristics in real rotating serpentine coolant flow passages which are very complex and three-dimensional, being affected by Coriolis and centrifugal forces combined with thermal buoyancy.

The mathematical model for steady heat conduction within an internally cooled turbine blade was represented by a boundary value problem over a multiply-connected domain resulting in a steady-state, nonlinear heat conduction equation. This equation was numerically integrated with the Boundary Element Method (BEM) because of its advantages over finite element and finite difference methods since the BEM did not require grid generation in the domain [7].

The thermal design engineer does not know in advance the temperature and heat flux distribu-

tions on the external turbine blade surface. We have observed [3] that an objective function based on integrated temperature difference is the most appropriate choice.

Here, the user specifies the desired average temperature within the material of the turbine blade. This temperature should be as high as possible while taking into account thermal creep and thermal cycle fatigue limitations of the material. The numerical optimization algorithm modified the geometry of the coolant passages in order to minimize the sum of squared differences between the local computed temperatures and the desired uniform temperature for each of the geometric perturbations.

We used a constrained evolutionary hybrid optimization approach [8, 3] in order to avoid local minimums. The hybrid algorithm incorporated: the Davidon-Fletcher-Powell (DFP) gradient search method, a genetic algorithm (GA), the Nelder-Mead (NM) method, and simulated annealing (SA). The new evolutionary hybrid scheme treated the existence of constraints in three ways: Rosen's projection method, a feasible search, and random design generation.

3 RESULTS

A turbine cascade airfoil shape (Fig. 2) with four coolant flow passages was chosen to simulate a typical airfoil. It was modeled as being made of stainless steel with thermal conductivity $k = 30.0 \text{ Wm}^{-1}\text{K}^{-1}$ and having a 150 microns thick thermal barrier coating with thermal conductivity, $k = 1.0 \text{ Wm}^{-1}\text{K}^{-1}$. For specified heat fluxes (Fig. 3) on the outside surface of the airfoil, the unstructured grid Navier-Stokes code predicted the corresponding surface temperature (Fig. 4) from which the heat convection coefficient distribution (Fig. 5) was obtained using inlet hot gas temperature as the ambient temperature. The desired average temperature in the entire airfoil was specified to be $\bar{T} = 1150 \text{ K}$. There were 20 geometric design variables in this test case: 8 vertices of the β -spline for the blade wall thickness, 2 strut x-locations/strut, 1 strut thickness/strut, and 1 filleting parameter (Lame curve exponent)/strut. Using this flexible geometry treatment of the interior of the airfoil and using the quasi conjugate heat transfer optimization, the four coolant flow passages converged to their new shapes and locations (Fig. 2). The cor-

responding temperature distribution on the airfoil outer surface was more uniform than the initial surface temperature distribution (Fig. 4). At the same time, the optimized coolant passages allowed for a significantly higher inlet hot gas temperature (Fig. 6). Evolution of the optimized coolant temperature, heat transfer coefficient, friction factor, surface roughness, and coolant flow rate are shown in Figs. 7-11. The entire design optimization process required three hours of a single processor time on Cray C-90 computer.

4 CONCLUSIONS

A method for computation of affordable optimization of coupled aerodynamics and heat transfer in internally cooled turbine airfoils has been developed and successfully demonstrated.

ACKNOWLEDGEMENTS

The authors are grateful for NASA-Penn State Space Propulsion Engineering Center Graduate Student Fellowship, National Science Foundation Grant DMI-9522854 monitored by Dr. George Hazelrigg, NASA Lewis Research Center Grant NAG3-1995 facilitated by Dr. John Lytle, and supervised by Dr. Kestutis Civinskas, and the ALCOA Foundation Faculty Research Fellowship facilitated by Dr. Yimin Ruan. Special thanks are due to Mr. Brian H. Dennis for his typesetting of this text.

REFERENCES

- [1] Dulikravich, G. S., Martin, T. J., Dennis B. H., Lee, E.-S., and Han, Z.-X. (May 1998) Aero-Thermo-Structural Design Optimization of Cooled Turbine Blades, AGARD - AVT Propulsion and Power Symposium in Design Principles and Methods for Aircraft Gas Turbine Engines, Editor: G. Meauze, Toulouse, France.
- [2] Han, Z.-X. and Liu, Z.-J. (November 1997) "Numerical Calculation of 2-D Inviscid Flow-Fields on Unstructured Grids", J. of Engineering Thermophysics, Vol. 18, No. 6.
- [3] Martin, T. J. and Dulikravich, G. S. (September 1997) "Aero-Thermal Analysis and Optimization of Internally Cooled Turbine Blades", XIII International Symposium on Airbreathing Engines (XIII ISABE), Chattanooga, TN, ISABE 97-7165, Vol. 2, pp. 1232-1250.
- [4] White, F. M. (1988) Heat and Mass Transfer, Addison-Wesley Publishing Company, Reading, MA, pp. 272.
- [5] Holman, J. P. (1981) "Heat Transfer", Fifth Edition, McGraw Hill Book Company.
- [6] Haaland, S. E., (March 1983) "Simple and Explicit Formulas for the Friction Factor in Turbulent Pipe Flows", Journal of Fluids Engineering, Vol. 105, pp. 89-90.
- [7] Dulikravich, G. S. and Martin, T. J. (1996) "Inverse Shape and Boundary Condition Problems and Optimization in Heat Conduction", Chapter 10 in Advances in Numerical Heat Transfer, Editors: W. J. Minkowycz and E. M. Sparrow, Taylor & Francis, pp. 324-367.
- [8] Foster, N. F. and Dulikravich, G. S. (January-February 1997) "Three-Dimensional Aerodynamic Shape Optimization Using Genetic and Gradient Search Algorithms", AIAA Journal of Spacecraft and Rockets, Vol. 34, No. 1, pp. 36-42.

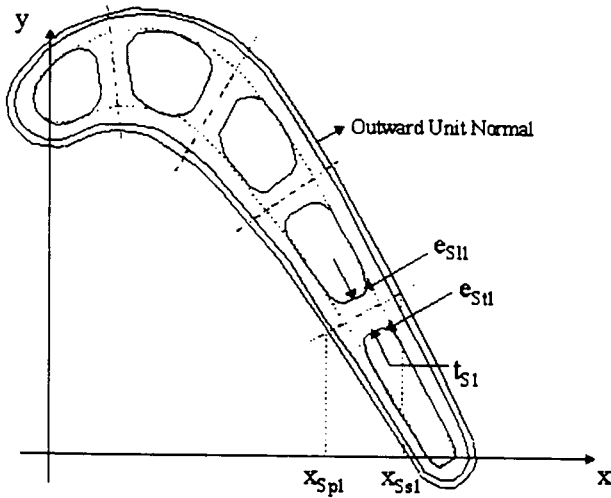


Figure 1. A flexible definition of turbine airfoil geometry with multiple coolant passages, struts, and a thermal barrier coating.

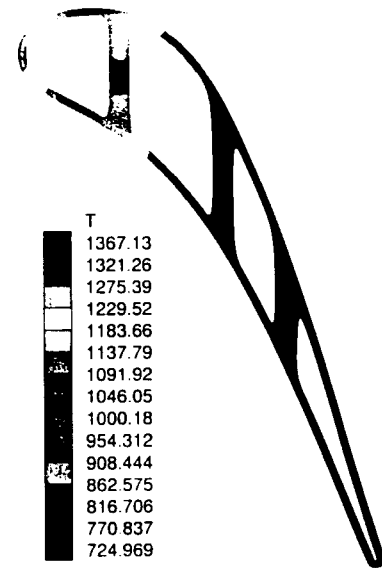


Figure 2. An example of the initial geometry of the interior for a coated internally cooled supersonic exit flow turbine airfoil.

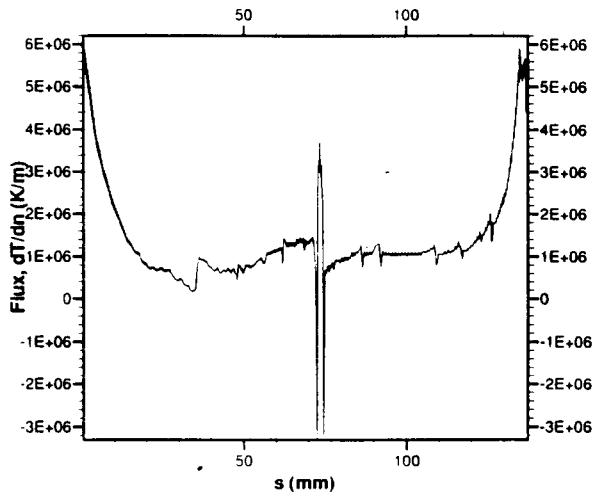


Figure 3. An example of initially specified normal temperature gradient distribution along the hot external surface.

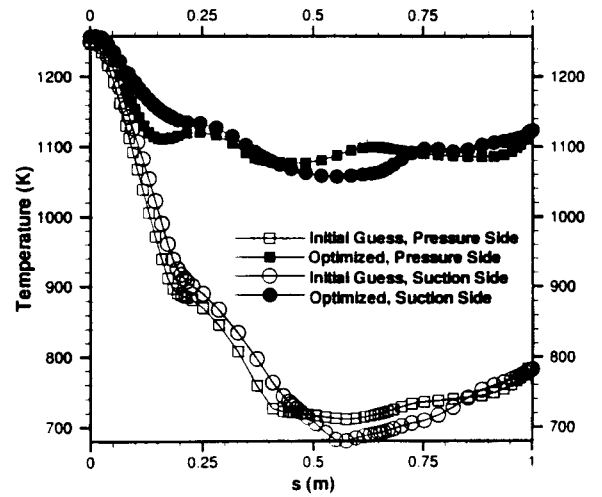


Figure 4. Corresponding temperature distribution on the external surface of the airfoil computed by a Navier-Stokes flow-field analysis code.

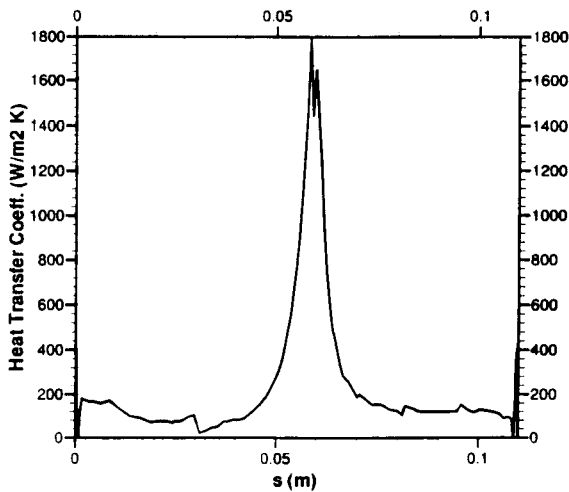


Figure 5. Heat transfer coefficient distribution on the external surface of the airfoil computed from the specified surface normal temperature derivatives, computed surface temperatures, and using turbine inlet static temperature as an ambient temperature.

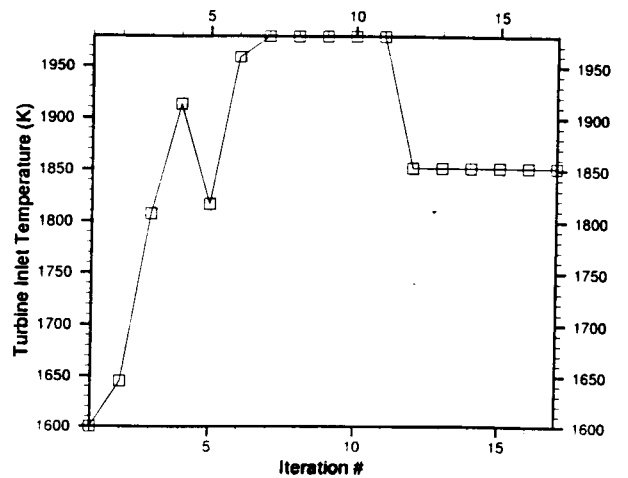


Figure 6. Turbine inlet hot gas static temperature maximization history during thermal optimization of the airfoil interior.

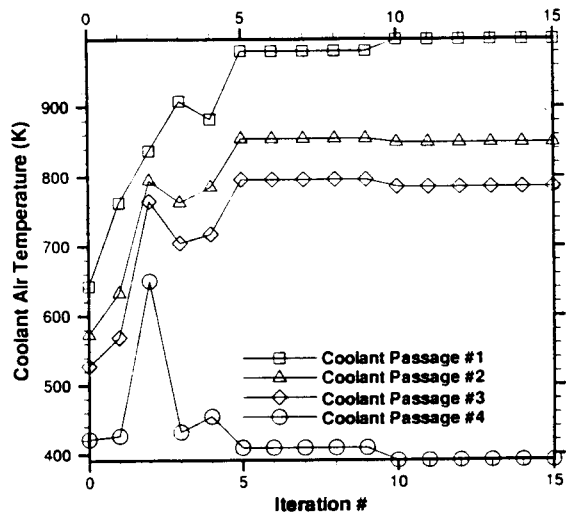


Figure 7. Coolant fluid temperature evolution history for each passage during thermal optimization of the airfoil interior

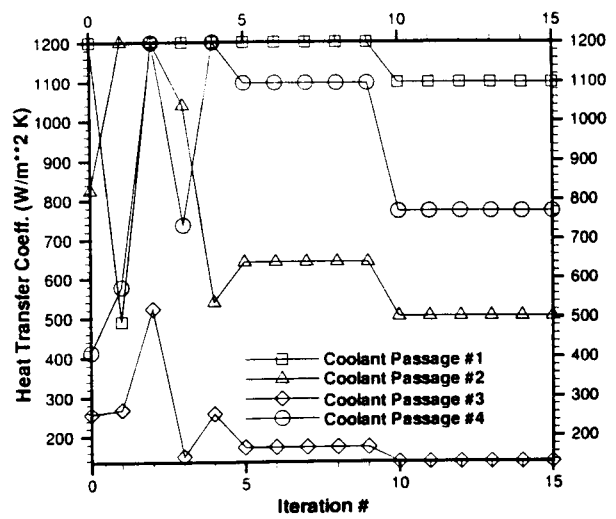


Figure 8. Heat transfer coefficient evolution history for each passage during thermal optimization of the airfoil interior

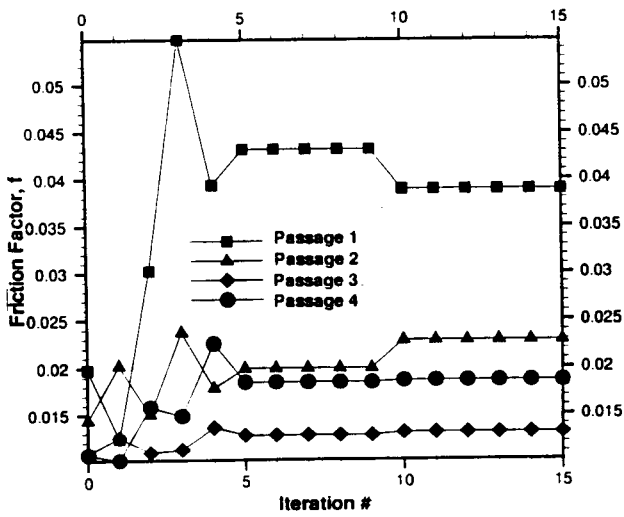


Figure 9. Friction factor evolution history for each passage during thermal optimization of the airfoil interior

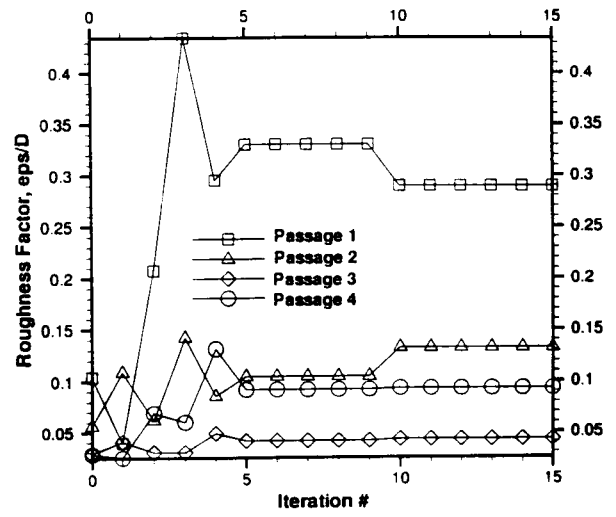


Figure 10. Relative surface roughness evolution history for each passage during thermal optimization of the airfoil interior

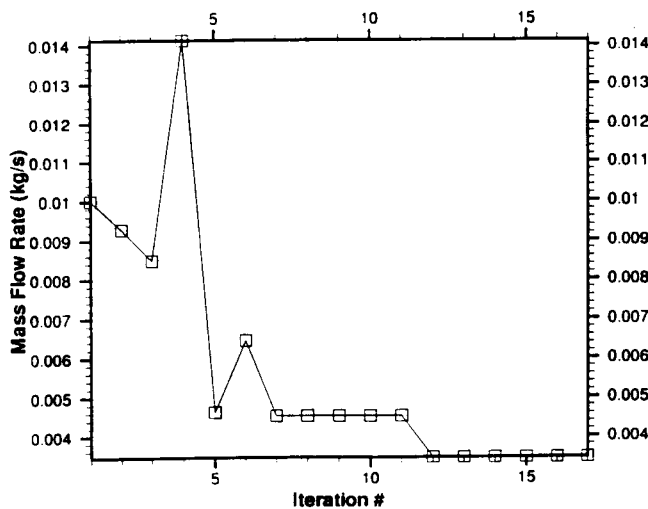


Figure 11. Coolant mass flow rate evolution history for each passage during thermal optimization of the airfoil interior